

# What can the SNO Neutral Current Rate teach us about the Solar Neutrino Anomaly

Abhijit Bandyopadhyay<sup>1</sup>, Sandhya Choubey<sup>1</sup>, Srubabati Goswami<sup>1</sup> and D.P. Roy<sup>2</sup>

<sup>1</sup>Saha Institute of Nuclear Physics, Bidhannagar, Kolkata 700 064, INDIA

<sup>2</sup>Tata Institute of Fundamental Research, Homi Bhabha Road, Mumbai 400 005, INDIA

## Abstract

We investigate how the anticipated neutral current rate from *SNO* will sharpen our understanding of the solar neutrino anomaly. Quantitative analyses are performed with representative values of this rate in the expected range of  $0.8 - 1.2$ . This would provide a  $5 - 10 \sigma$  signal for  $\nu_e$  transition into a state containing an active neutrino component. Assuming this state to be purely active one can estimate both the  ${}^8B$  neutrino flux and the  $\nu_e$  survival probability to a much higher precision than currently possible. Finally the measured value of the *NC* rate will have profound implications for the mass and mixing parameters of the solar neutrino oscillation solution.

A large number of experiments have observed anomalously low solar neutrino flux [1-4] compared to the standard solar model (SSM) prediction [5]. They are the radiochemical experiments on *Ga* [1] and *Cl* [2] targets as well as the water Cerenkov experiments from Super Kamiokande (SK) [3] and Sudbury Neutrino Observatory (*SNO*) [4]. SK observes the emitted electron from elastic scattering

$$\nu + e \rightarrow \nu + e, \quad (1)$$

while *SNO* observes it from the charged current process

$$\nu_e + d \rightarrow p + p + e \quad (2)$$

using a heavy water target. Both the experiments probe the high energy tail of the solar neutrino spectrum, which is dominated by the  ${}^8B$  neutrino flux. The SK elastic scattering process (1) is sensitive to  $\nu_e$  via CC and NC interactions; but it also has a limited sensitivity to  $\nu_{\mu,\tau}$  via the NC interaction. On the other hand the *SNO* experiment is looking separately at the NC rate, which has equal sensitivity to all the active neutrino flavours, via

$$\nu + d \rightarrow \nu + p + n, \quad (3)$$

followed by the neutron capture by *NaCl*. The resulting excited state decays via  $\gamma$  emission, which constitutes the NC signal. The *SNO* experiment is expected to report its first NC rate shortly, corresponding to a data sample of  $\sim 10^3$  events – i.e. similar statistical accuracy as their 1st CC data [4]. The purpose of our work is to critically analyse how far this data will enhance our understanding of the solar neutrino anomaly and its solution.

By far the most plausible solution of the solar neutrino anomaly is in terms of neutrino oscillation, and in particular the oscillation of  $\nu_e$  into another active flavour  $\nu_a$ , which can be any combination of  $\nu_\mu$  and  $\nu_\tau$ . Indeed we have made considerable progress in understanding the solar neutrino anomaly and its oscillation solution over the past few months by combining the CC rate from *SNO* with the SK elastic scattering data [6-9]. Firstly they disfavour  $\nu_e$  transition into a sterile neutrino  $\nu_s$  at the  $3\sigma$  level in a model independent way [4]. Secondly, assuming only transition between  $\nu_e$  and  $\nu_a$ , one can estimate both the  ${}^8B$  flux and the  $\nu_e$  survival probability, although with fairly large uncertainties [7]. Thirdly one can do a combined analysis of the *SNO*, *SK* and the earlier radiochemical data assuming SSM and the  $\nu_e \rightarrow \nu_a$  oscillation model [7-9]. One sees that the result has narrowed down to only two possible solutions, both having large mixing angles – i.e. the so called LMA and LOW solutions. We shall see below that each of the above results can be significantly sharpened further by including the NC rate from *SNO*.

Table 1 lists the observed solar neutrino rates of the *Ga*, *Cl*, *SK* and *SNO* (CC) experiments relative to the corresponding SSM predictions. The compositions of the respective solar neutrino fluxes are also indicated along with the threshold energies. Assuming the SSM neutrino fluxes and the transition of  $\nu_e$  into an active flavour  $\nu_a$  one can write the SK elastic scattering rate relative to the SSM prediction in terms the survival probability, i.e.

$$R_{SK}^{el} = P_{ee} + rP_{ea} = P_{ee} + r(1 - P_{ee}), \quad (4)$$

where  $r = \sigma_{\nu_a}^{NC} / \sigma_{\nu_e}^{CC+NC} \simeq 0.17$  is the ratio of  $\nu_{\mu,\tau}$  to  $\nu_e$  elastic scattering cross-sections [6]. The resulting value of the  $\nu_e$  survival probability  $P_{ee}$  is shown paranthetically in Table 1. The other rates shown in this table are identical to the corresponding  $P_{ee}$ , since they are sensitive to  $\nu_e$  only.

As we see from table 1, the *SK* and *SNO* experiments are sensitive only to the  ${}^8B$  neutrino spectrum. While the shape of this spectrum is predicted with good precession by the SSM, there is a large uncertainty in the predicted normalisation [5],

$$\phi_B = 5.05 \times 10^6 \left(1_{-0.16}^{+0.20}\right) cm^{-2}s^{-1}, \quad (5)$$

arising from the uncertainty in the  ${}^7Be + p \rightarrow {}^8B + \gamma$  cross-section. Therefore we shall introduce a constant parameter  $f_B$  to denote the normalisation of the  ${}^8B$  neutrino flux relative to the SSM prediction. Then the SK elastic scattering and the *SNO* *CC* and *NC* scattering rates relative to the corresponding *SSM* predictions are

$$R_{SK}^{el} = f_B P_{ee} + f_B r P_{ea}, \quad (6)$$

$$R_{SNO}^{CC} = f_B P_{ee}, \quad (7)$$

$$R_{SNO}^{NC} = f_B (P_{ee} + P_{ea}), \quad (8)$$

which hold for the general case of  $\nu_e$  transitoin into any combination of  $\nu_a$  and  $\nu_s$ . It should be noted here that these three measurements do not have identical energy ranges. The *SK* and *SNO* *CC* data start from neutrino energies of 5 and 7 MeV respectively, while the response function of the *SNO* *NC* measurement extends marginally below 5 MeV. However the SK rate and the resulting survival probability show energy independence down to 5 MeV to a very good precession. The *SNO* *CC* rate shows energy independence as well, although to lesser precession. Therefore it is reasonable to assume a common survival probability for all the three measurements.

As recently discussed in [6], the SK elastic and the *SNO* *CC* rates can be combined to access information on *NC* scattering, so that in principle there is no new information contained in the *SNO* *NC* rate. In fact eqs. (6,7,8) can be seen to give the sum rule

$$R_{SNO}^{NC} = R_{SNO}^{CC} + (R_{SK}^{el} - R_{SNO}^{CC})/r, \quad (9)$$

which predicts  $R_{SNO}^{NC} = 1.0 \pm 0.24$  [6]. However the large uncertainty in this prediction reflects the low sensitivity of  $R_{SK}^{el}$  to *NC* scattering, which is weighted by a small coefficient  $r$ . On the other hand the expected *NC* scattering rate from *SNO* at the level of  $\sim 10^3$  events should have a similar precession as their present CC rate, i.e.  $\pm 8\%$ , which will ultimately go up to  $\pm 5\%$ . Keeping in mind the predicted range of  $R_{SNO}^{NC}$  we shall assume

$$R_{SNO}^{NC} = 1.0 \pm .08, 1.2 \pm .08, 0.8 \pm .08 \quad (10)$$

as three representative values of the *NC* scattering rate expected from *SNO* and analyse the implications for the solar neutrino anomaly. We shall see below that the  $R_{SNO}^{NC}$  input will lead to qualitative improvement in the results of all the three types of analyses mentioned earlier.

**General Analysis of  $\nu_e \rightarrow \nu_{a,s}$  Transitions:** Let us start with a model independent analysis of  $\nu_e$  transition into an active neutrino flavour  $\nu_a$ . One sees from eqs. (6,7) that the observed excess of  $R_{SK}^{el}$  over the  $R_{SNO}^{CC}$  in Table 1 constitutes a  $3\sigma$  signal for  $\nu_e \rightarrow \nu_a$  transition i.e. transition of  $\nu_e$  into a state of atleast partly active neutrino, or equivalently a  $3\sigma$  signal against a pure  $\nu_e \rightarrow \nu_s$  transition [4]. Similarly an observed excess of  $R_{SNO}^{NC}$  (8) over  $R_{SNO}^{CC}$  (7) will constitute a model independent signal for the  $\nu_e \rightarrow \nu_a$  transition  $P_{ea}$ . Fig. 1 compares the  $R_{SNO}^{NC}$  values of eq. (10) with the current value of  $R_{SNO}^{CC}$ . It shows that an observed value of  $R_{SNO}^{NC}$  in the range of  $0.8 - 1.2(\pm 0.08)$  will constitute of  $5 - 10 \sigma$  signal for  $\nu_e \rightarrow \nu_a$  transition.

Unfortunately one cannot get a model independent estimate of the  $\nu_e \rightarrow \nu_a$  transition probability  $P_{ea}$ , since the above excess corresponds to the product  $f_B P_{ea}$ . In fact it is evident from eqs. (6-8) that these two quantities can not be separated with or without the  $P_{SNO}^{NC}$  input. In other words for the general case of  $\nu_e$  transition into a mixture of active and sterile neutrinos,

$$\nu_a \sin \alpha + \nu_s \cos \alpha, \quad (11)$$

one can rewrite eqs. (6) and (8) as

$$R_{SK}^{el} = f_B P_{ee} + f_B r \sin^2 \alpha (1 - P_{ee}), \quad (12)$$

$$R_{SNO}^{NC} = f_B P_{ee} + f_B \sin^2 \alpha (1 - P_{ee}). \quad (13)$$

Then it will not be possible to separately estimate the parameters  $f_B$  and  $\sin^2 \alpha$ . One can only determine the following combination in two different ways, i.e.

$$\sin^2 \alpha (f_B - R_{SNO}^{CC}) = (R_{SK}^{el} - R_{SNO}^{CC})/r, \quad (14)$$

$$\sin^2 \alpha (f_B - R_{SNO}^{CC}) = R_{SNO}^{NC} - R_{SNO}^{CC}. \quad (15)$$

A two parameter fit to (14) was done in ref. [6] to determine the allowed contour in the  $f_B - \sin^2 \alpha$  plane. We shall instead treat  $\sin^2 \alpha$  as a model parameter. And for each input value of  $\sin^2 \alpha$  we shall determine  $f_B$  first from eq. (14) and then from a weighted average of eqs. (14) and (15). The results are shown as lines corresponding to the central value of  $f_B$  along with the  $1\sigma$  and  $2\sigma$  boundaries in the  $f_B - \sin^2 \alpha$  plane in Figs. 2 and 3. The advantage of this procedure is that for  $\sin^2 \alpha = 1$  the  $1\sigma$  and  $2\sigma$  ranges of  $f_B$  shown correspond to those of the pure  $\nu_e \rightarrow \nu_a$  transition model without any sterile neutrino, which would not be the case for the two parameter fit [6].

A comparison of Figs. 2 and 3 shows the enormous improvement in precision one expects by including the  $NC$  rate from  $SNO$ . The vertical lines indicate the  $2\sigma$  limits on  $f_B$  from the SSM. Combining the two limits one could rule out models having  $\sin^2 \alpha < 0.3$  (i.e. singlet neutrino component  $\cos^2 \alpha > 0.7$ ) at  $2\sigma$  level for  $R_{SNO}^{NC} = 0.8 \pm 0.08$ , while  $R_{SNO}^{NC} = 1.2 \pm 0.08$  would rule out all those singlet neutrino models with  $\sin^2 \alpha < 0.6$  ( $\cos^2 \alpha > 0.4$ ). However within the present uncertainty of the  $SSM$  value of the  $^8B$  neutrino flux it is unlikely to rule out models with a  $\nu_s$  component  $\cos^2 \alpha < 0.3$ . Nor is it likely to set any upper limit on  $\sin^2 \alpha$ , which would show incompatibility with pure  $\nu_e \rightarrow \nu_a$  transition.

**Analysis of pure  $\nu_e \rightarrow \nu_a$  Transition:** Assuming no sterile neutrino the eqs. (6) and (8) reduce to

$$R_{SK}^{el} = f_B P_{ee} + f_B r(1 - P_{ee}), \quad (16)$$

$$R_{SNO}^{NC} = f_B. \quad (17)$$

In this case it is possible to estimate both  $f_B$  and  $P_{ee}$  from the  $SK$  elastic and the  $SNO$   $CC$  rates even without the  $NC$  rate from  $SNO$  [7]. Fig. 4 shows the 1 and 2 sigma contours of this solution along with the corresponding ones obtained by including the  $R_{SNO}^{NC}$  input. Our result in the former case is in good agreement with that of ref. [7], although the two methods are not identical. Thanks to the effective energy independence of the survival probability the result is insensitive to the difference between the energy thresholds of the  $SK$  elastic and the  $SNO$   $CC$  rates. Unfortunately the resulting  $f_B$  has large error, which reflects the low sensitivity of  $R_{SK}^{el}$  to  $f_B$  (eq. 16). Interestingly both the central value and the error bar of  $f_B$  are practically the same as those of the  $SSM$  (shown for comparison near the right scale). The error in  $f_B$  propagates into  $P_{ee}$  due to a strong anticorrelation between the two quantities as their product is well constrained by  $R_{SNO}^{CC}$  (7). Fig. 4 shows that the inclusion of the  $NC$  rate from  $SNO$  will result in a reduction in the uncertainty of the  ${}^8B$  neutrino flux  $f_B$  and the corresponding survival probability  $P_{ee}$  by about a factor of 2.5.

**The  $\nu_e \rightarrow \nu_a$  oscillation solutions to the Solar Neutrino Anomaly:** Finally we shall fit the global solar neutrino data with a standard two-family ( $\nu_e \rightarrow \nu_a$ ) oscillation model assuming the  $SSM$  fluxes, but with one difference. Instead of  $R_{SK}^{el}$  and  $R_{SNO}^{CC}$  we shall fit the ratios  $R_{SK}^{el}/R_{SNO}^{NC}$  and  $R_{SNO}^{CC}/R_{SNO}^{NC}$ . As we see from eqs. (7,16,17) the  ${}^8B$  neutrino flux  $f_B$  factors out from these two ratios. Thus the result becomes immune to the large uncertainty in the  $SSM$  value of the  ${}^8B$  neutrino flux (5). We shall include the 19 + 19 day-night spectral points from  $SK$ , but with free normalisation to avoid double counting [7,8,10]. We shall also include the combined  $Ga$  rate of Table 1 in the fit. However we shall exclude the  $Cl$  rate, since the experiment has not been independently calibrated. Besides the apparent rise of the  $CC$  rate between the  $Cl$  and  $SK/SNO$  energies is in conflict with the  $LMA$  and  $LOW$  solutions, which are strongly favoured by the global fit [10]. Fig. 5 shows the 90%, 95%, 99% and 99.73% ( $3\sigma$ )  $CL$  contours of the fits for the three representative values of  $R_{SNO}^{NC}$  (10), which is the same as  $f_B$  (eq. 17). We have checked that all the three fits have equally good  $\chi^2_{\min}$ . ( $\sim 30$ ) and goodness of fit ( $\sim 80\%$ ).

The left panel of Fig. 5 represents  $R_{SNO}^{NC} = f_B = 0.8 \pm .08$ . It corresponds to enhancing the survival probability  $P_{ee}$  at  $SK/SNO$  from 0.35 to nearly 0.45, while  $P_{ee}$  at  $Ga$  energy goes up by only 2%. Thus the energy dependence of  $P_{ee}$  between the  $Ga$  and  $SK/SNO$  energies become very mild. Consequently the solution favours large mixing angle, going upto maximal mixing, where it remains valid over two large mass ranges around  $\delta m^2 = 10^{-4}$  eV<sup>2</sup> and  $10^{-7}$  eV<sup>2</sup> [10]. These are the so-called  $LMA$  and  $LOW$  solutions. In the present context however it will be more appropriate to call them  $HIGH$  and  $LOW$  solutions, since both of them correspond to large mixing angles. The middle panel represents  $R_{SNO}^{NC} = f_B = 1.0 \pm .08$ , which means that the survival probability  $P_{ee}$  at  $Ga$  and  $SK/SNO$

energies corresponds to those shown in Table 1. Since such a large energy dependence cannot be explained by the earth matter effect, the *LOW* solution is only allowed at the  $3\sigma$  level. On the other hand the *HIGH* solution occurs at the upper edge of the *MSW* region in  $\delta m^2/E$ . Thus the survival probability goes down from  $P_{ee} \simeq 1 - \frac{1}{2} \sin^2 2\theta > 0.5$  above the *MSW* region to  $P_{ee} \simeq \sin^2 \theta$  inside it as one moves up from *Ga* to *SK/SNO* energies [10]. The right panel corresponds to  $R_{SNO}^{NC} = f_B = 1.2 \pm .08$ , which means that the survival probability at *SK/SNO* energies goes down further by a factor of 1.2. Consequently the *LOW* solution disappears completely while the *HIGH* solution moves to a lower mixing angle. Thus the measured value of the *NC* rate at *SNO* can have a profound effect on the mass and mixing angle of the solar neutrino oscillation solution.

### Summary:

In anticipation of the first *NC* rate from *SNO* we have analysed how this data will sharpen our understanding of the solar neutrino anomaly. For a quantitative analysis we have chosen three representative value of this rate,  $R_{SNO}^{NC} = 0.8, 1.0$  and  $1.2(\pm .08)$ . They span the  $\pm 1\sigma$  range of this quantity as estimated from the *SK* elastic and *SNO CC* rates. The main results are listed below.

1. It will provide a  $5 - 10\sigma$  signal for  $\nu_e$  transition into an active flavour  $\nu_a$  (or against a pure  $\nu_e$  transition into a sterile neutrino  $\nu_s$ ).
2. However for transition into a mixture of  $\nu_a$  and  $\nu_s$ , we need to know the  ${}^8B$  neutrino flux to constrain the size of the sterile component. If we assume the *SSM* prediction for this flux then  $R_{SNO}^{NC} = 1.2 \pm .08$  ( $0.8 \pm .08$ ) would imply the sterile component to be  $< 40\%$  ( $70\%$ ) at the  $2\sigma$  level.
3. Assuming a pure  $\nu_e \rightarrow \nu_a$  transition one can combine  $R_{SNO}^{NC}$  with  $R_{SNO}^{CC}$  and  $R_{SK}^{el}$  to determine both the  ${}^8B$  neutrino flux and the  $\nu_e$  survival probability to much higher precision than is possible now from the latter two data.
4. Finally one can do a  $\nu_e \rightarrow \nu_a$  oscillation model fit to the global solar neutrino data assuming the *SSM* fluxes, but replacing the  $R_{SK}^{el}$  and  $R_{SNO}^{CC}$  by the ratios  $R_{SK}^{el}/R_{SNO}^{NC}$  and  $R_{SNO}^{CC}/R_{SNO}^{NC}$ , which are independent of the  ${}^8B$  neutrino flux. For  $R_{SNO}^{NC} = 0.8 \pm .08$  we get both the *LMA* (*HIGH*) and *LOW* solutions covering large ranges of mass and mixing angle, including maximal mixing. On the other hand  $R_{SNO}^{NC} \geq 1$  strongly disfavours the *LOW* solution, while the *HIGH* solution is restricted to a small patch in mass and mixing angle excluding maximal mixing. Thus the measured value of  $R_{SNO}^{NC}$  can have a profound effect on the mass and mixing parameters of the solar neutrino oscillation.

We thank S. Umasankar for discussions.

## References

1. GNO Collaboration: M. Altmann et al., Phys. Lett. B490, 16 (2000); Gallex Collaboration: W. Hampel et al., Phys. Lett. B447 (1999); SAGE Collaboration: J.N. Abdurashitov et al., Phys. Rev. C60, 05580 (1999).
2. B.T. Cleveland et al., Astrophys. J. 496, 505 (1998).
3. S.K. Collaboration: S. Fukuda et al., hep-ex/0103032.
4. SNO Collaboration: Q.R. Ahmad et al., Phys. Rev. Lett. 87, 071301 (2001).
5. J.N. Bahcall, M.H. Pinsonneault and S. Basu, Astrophys. J. 555, 990 (2001).
6. V. Barger, D. Marfatia and K. Whisnant, Phys. Rev. Lett. 88, 011302 (2002).
7. G.L. Fogli, E. Lisi, D. Montanino and A. Palazzo, Phys. Rev. D64, 093007 (2001).
8. A. Bandyopadhyay, S. Choubey, S. Goswami and K. Kar, Phys. Lett. B519, 83 (2001); S. Choubey, S. Goswami and D.P. Roy, Phys. Rev. D65, 073001(2002); A. Bandyopadhyay, S. Choubey, S. Goswami and K. Kar, hep-ph/0110307(to be published in Phys. Rev. D); P. I. Krastev and A. Y. Smirnov, hep-ph/0108117.
9. J.N. Bahcall, M.C. Gonzalez-Garcia and C. Pena-Garay, JHEP 0108, 014 (2001); J.N. Bahcall, M.C. Gonzalez-Garcia and C. Pena-Garay, hep-ph/0111150.
10. S. Choubey, S. Goswami, N. Gupta and D.P. Roy, Phys. Rev. D64, 053002 (2001).

Table 1. The observed solar neutrino rates relative to the  $SSM$  predictions are shown along with their compositions and threshold energies for different experiments. For the  $SK$  experiment the  $\nu_e$  contribution to the rate  $R$  is shown in parantheses assuming  $\nu_e \rightarrow \nu_a$  transition.

experiment	$R$	composition	$E_{th}$ (MeV)
$Ga$	$0.584 \pm 0.039$	$pp(55\%), Be(25\%), B(10\%)$	0.2
$Cl$	$0.335 \pm 0.029$	$B(75\%), Be(15\%)$	0.8
$SK$	$0.459 \pm 0.017$ ( $0.351 \pm 0.017$ )	$B(100\%)$	5.0
$SNO(CC)$	$0.347 \pm 0.027$	$B(100\%)$	7.0



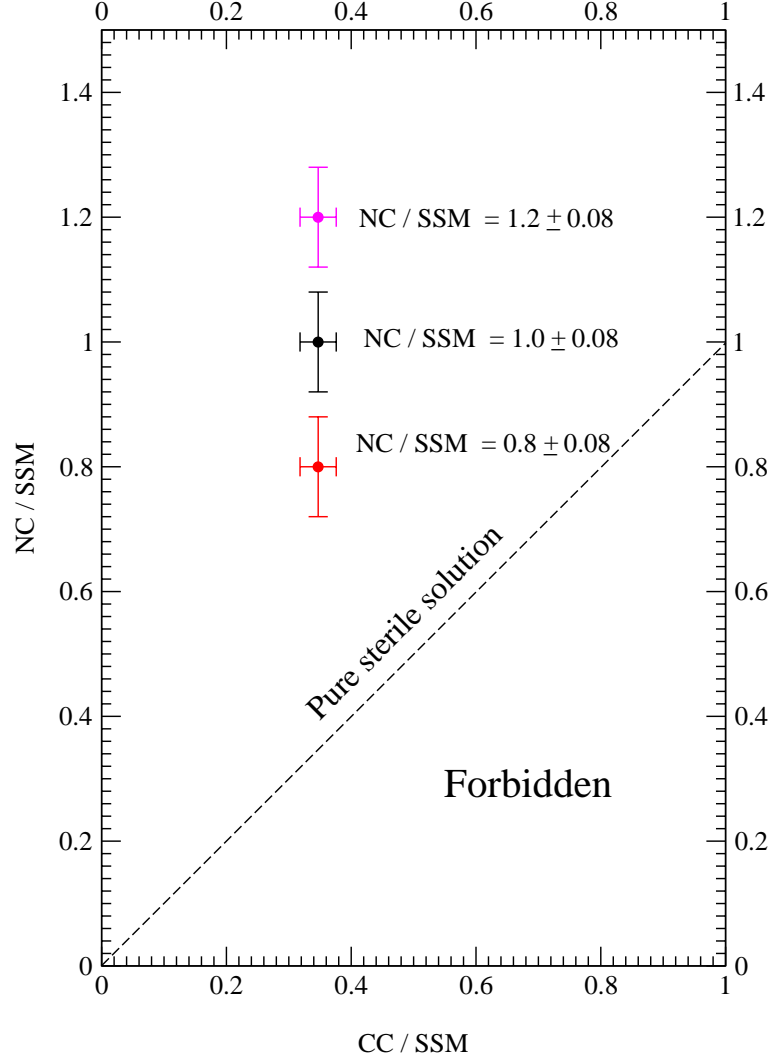


Figure 1: The *SNO* *CC* and *NC* rates shown relative to their *SSM* predictions for the three representative values of the latter. The dashed line is the prediction of the pure  $\nu_e$  to  $\nu_s$  transition.

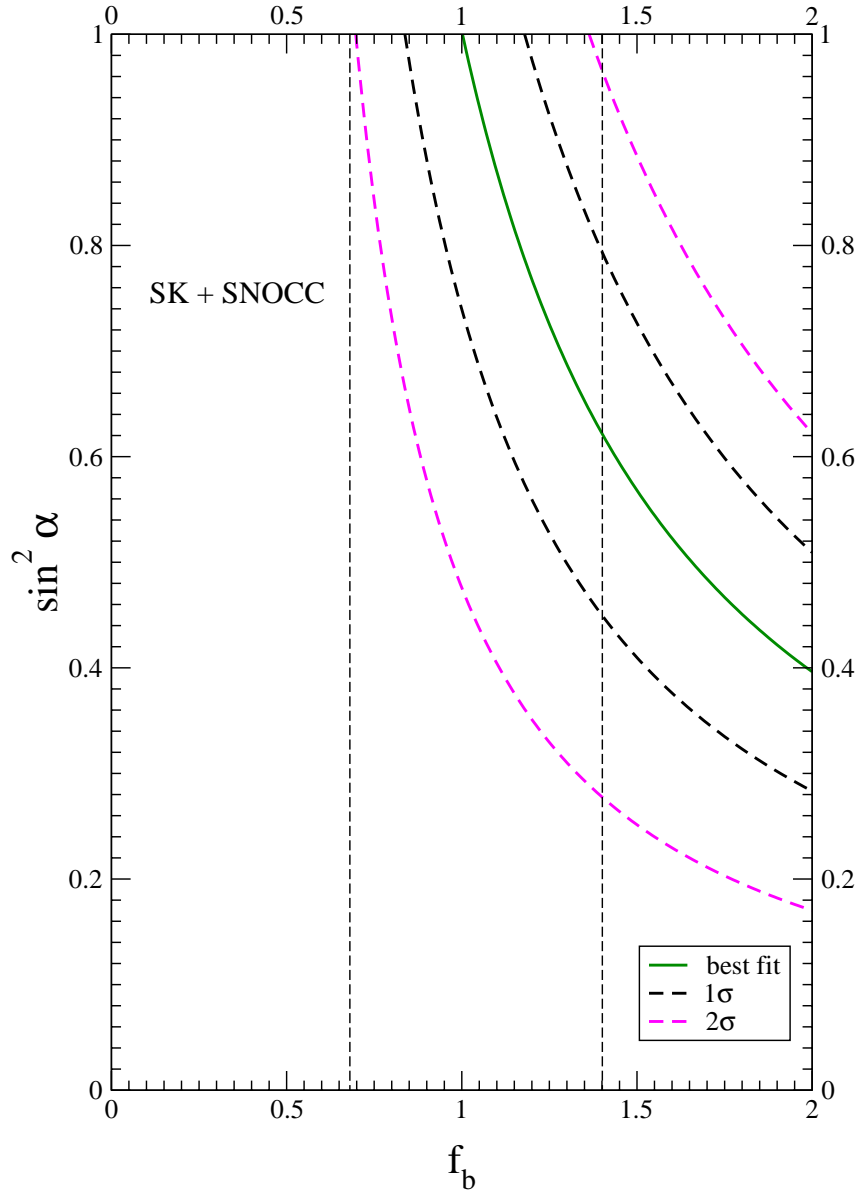


Figure 2: Best fit value of the  ${}^8B$  neutrino flux shown along with the  $1\sigma$  and  $2\sigma$  limits against the model parameter  $\sin^2 \alpha$ , representing  $\nu_e$  transition into a mixed state ( $\nu_a \sin \alpha + \nu_s \cos \alpha$ ). The dashed line denote the  $\pm 2\sigma$  limits of the *SSM*.

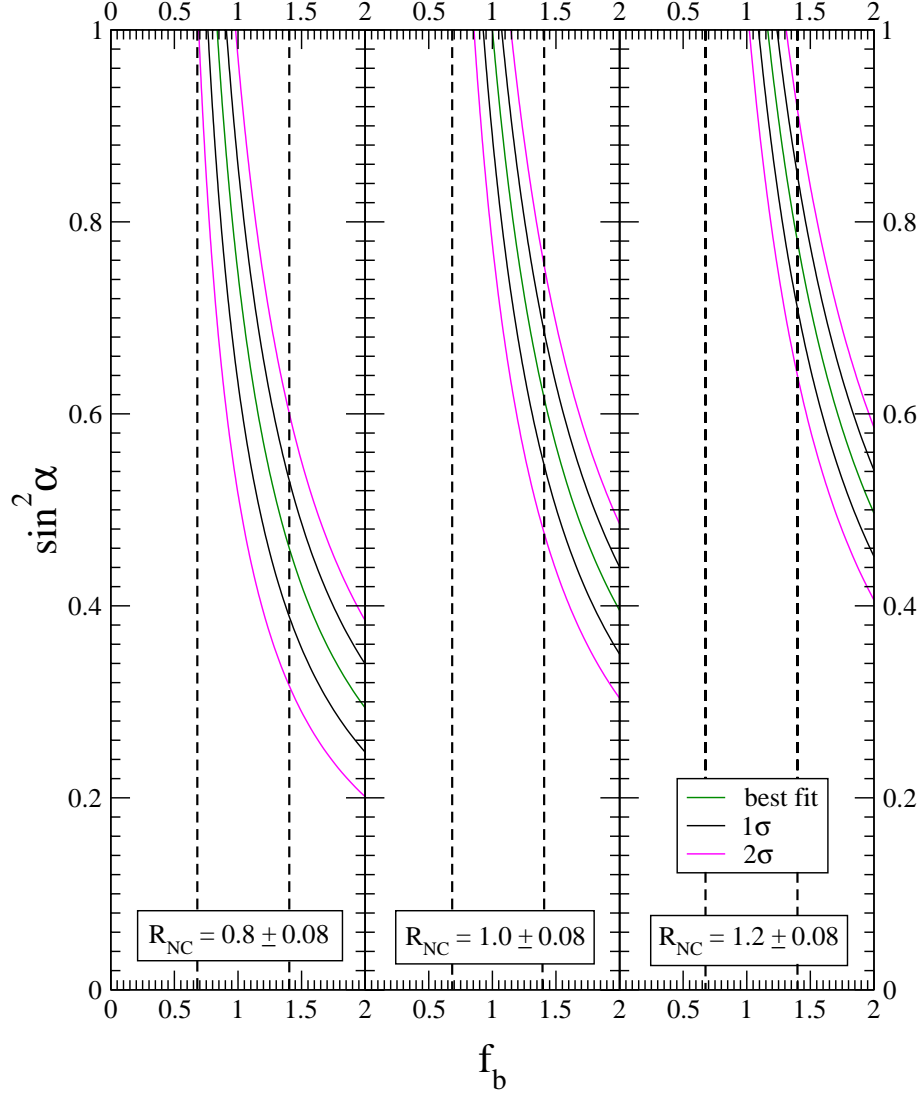


Figure 3: Same as Fig. 2 but including the  $NC$  rate to the fit along with the  $SK$  elastic and  $SNO$   $CC$  rates. The dashed lines denote the  $\pm 2\sigma$  limits of the  $SSM$ .

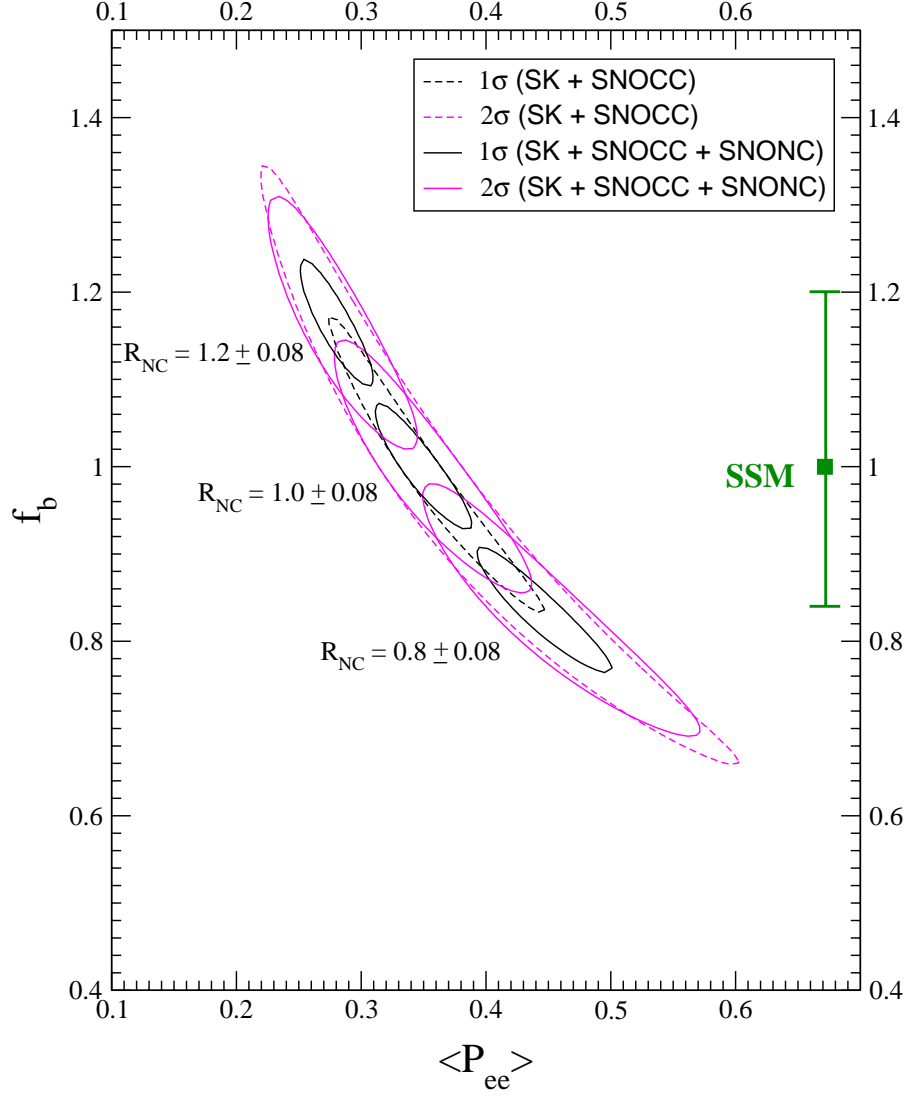


Figure 4: The 1 and 2 $\sigma$  contours of solutions to the  $^8B$  neutrino flux  $f_B$  and the  $\nu_e$  survival probability  $P_{ee}$  assuming  $\nu_e$  to  $\nu_a$  transition. The size of the *SSM* error bar for  $f_B$  is indicated on the right.

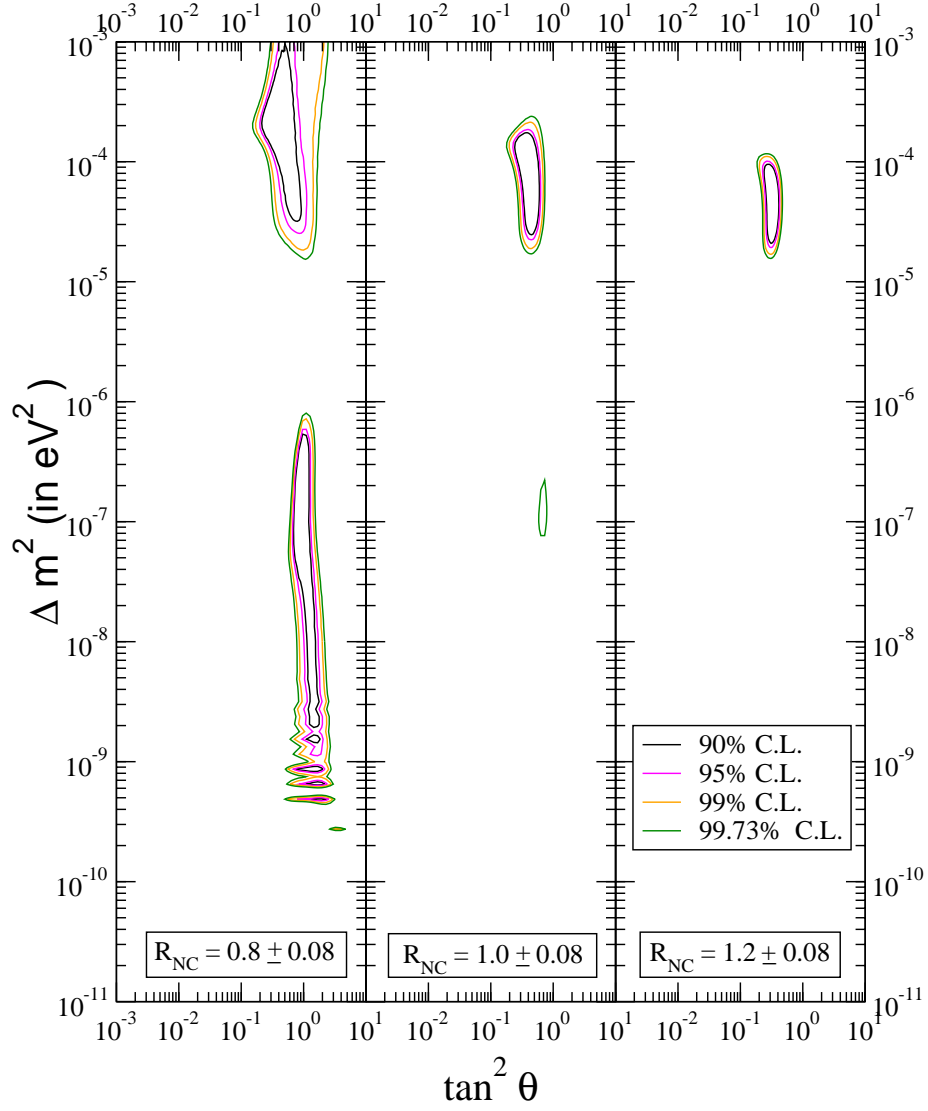


Figure 5: The  $\nu_e \rightarrow \nu_a$  oscillation solutions to the *Ga* rate, *SK* day-night energy spectra along with the *SK* and *SNO* (*CC*) rates, both normalised by the *SNO* (*NC*) rate.